Sufentanil combined with parecoxib sodium inhibits breast cancer proliferation and metastasis via regulating epithelial-mesenchymal transition in HER2-positive breast cancer cells

Sunmian Xu
Ningxia Medical University
Xiaohui Li
General Hospital of Ningxia Medical University
Wenbin Li
General Hospital of Ningxia Medical University
Nina Ma
General Hospital of Ningxia Medical University
Hongjun Ma
General Hospital of Ningxia Medical University
Jian Cui
General Hospital of Ningxia Medical University
Xiaogang You
General Hospital of Ningxia Medical University
Xuexin Chen (chenxuexin2637@163.com)
General Hospital of Ningxia Medical University

Research Article

Keywords: sufentanil, parecoxib sodium, HER2-positive breast cancer, proliferation, metastasis, epithelial-mesenchymal transition

Posted Date: July 21st, 2022

DOI: https://doi.org/10.21203/rs.3.rs-1853361/v1

Additional Declarations: No competing interests reported.

Version of Record: A version of this preprint was published at Clinical & Experimental Metastasis on February 18th, 2023. See the published version at https://doi.org/10.1007/s10585-023-10199-6.

Abstract

Background: Sufentanil combined with parecoxib sodium is a commonly used combination of postoperative anesthetic analgesics in perioperative oncology patients. However, the effects on HER2-positive breast cancer cells are still unknown. The aim of this study was to investigate the effects and potential mechanisms of sufentanil combined with parecoxib sodium on HER2-positive breast cancer cells.

Methods: Cell proliferation, cycle, migration and invasion abilities were assessed by CCK-8 assay, plate clone formation assay, flow cytometric cycle assay, scratch and transwell invasion assays, and Western blot assay was used to detect the expression of proteins involved in cell cycle, migration, invasion and epithelial-mesenchymal transition (EMT)-related proteins. The effect of tumor growth and metastasis *in vivo* was examined by constructing an orthotopic transplantation model of HER2-positive breast cancer in mice.

Results: Functional assays indicated that sufentanil combined with parecoxib sodium induced blockade of HER2-positive breast cancer cells BT474 in the G1 phase of the cell cycle and inhibited cell proliferation, migration and invasion *in vitro*. Western blot assays revealed that sufentanil combined with parecoxib sodium down-regulated the expression of Cyclin D1, MMP-9, MMP-2 and VEGFA proteins in BT474 cells, as well as the expression of mesenchymal phenotypic proteins N-cadherin, Vimentin and Snail, while upregulated the expression of epithelial phenotypic protein E-cadherin. In addition, we found that sufentanil combined with parecoxib sodium inhibited tumor growth and metastasis in a recipient mice model.

Conclusion: Sufentanil combined with parecoxib sodium inhibits HER2-positive breast cancer disease progression, including cell proliferation, cycle, migration, and invasion, and this alteration is associated with EMT.

1. Introduction

According to the Global Cancer Report 2020 [1], breast cancer has officially replaced lung cancer as the largest cancer in the world, with human epidermal growth factor receptor 2 (HER2)-positive patients accounting for approximately 20%-30%. Compared to other subtypes of breast cancer, HER2-positive breast cancer patients have a shorter time to recurrence and overall survival [2]. Despite significant improvements in the treatment of breast cancer compared to the last century, postoperative metastasis and recurrence have become the main cause of patient prognosis [3,4].

Studies have shown that the perioperative period is an important "window period" for metastasis and recurrence in tumor patients [5,6], in which anesthesia plays an important role [7,8]. It is believed that the use of anesthetic drugs can have long-term effects on the body [9]. At the same time, the pain and inflammatory response caused by surgical trauma together promote the growth of tumor cells and inhibit

their clearance by the body [10,11]. Therefore, the use of reasonable anesthetic drug regimens to exert analgesia, suppress excessive inflammatory responses and improve the body's immune function can reduce the metastasis and recurrence of tumor cells.

Sufentanil and parecoxib sodium are not only widely used in numerous hospitals [12], but the combination is also a classical pairing regimen for postoperative analgesia [13]. However, there is no consensus on the study of the effects of sufentanil on tumor metastasis and recurrence, and there are still many questions and debates to be resolved [14-16]. Parecoxib sodium, a commonly used selective inhibitor of COX-2, not only exerts anti-inflammatory and analgesic effects, but also has potential antitumor effects [17]. Encouragingly, prognostic studies of sufentanil in combination with NSAIDs-like drugs in tumor patients have also shown to have the ability to reduce the risk of postoperative metastasis and recurrence in tumor patients, and are considered a feasible approach to enhance the efficacy and improve the prognosis of tumor patients [18-20].

There are limited basic research on the effects of sufentanil combined with parecoxib sodium on tumor cell metastasis and recurrence, and even less in HER2-positive breast cancer. Therefore, in this study, we investigated the effects of sufentanil combined with parecoxib sodium on the proliferation and metastatic ability of HER2-positive breast cancer cells at the cellular and animal levels, and preliminarily explored the mechanisms of the effects. The aim is to reveal the anti-tumor potential of perioperative sufentanil combined with parecoxib sodium in the treatment of breast cancer, and also to provide a theoretical basis for the clinical selection of an appropriate anesthetic analgesic regimen.

2. Materials And Methods

2.1 Cell culture and animal feeding

BT474 breast cancer cells (Cell bank of Chinese Academy of Sciences, China) were cultured in RPMI-1640 medium (Gibco, 31870074, USA) containing 10% fetal bovine serum (FBS) (Gibco,12483020, USA) and 1% penicillin (Beijing Solarbio Technology Co., Ltd, 10378016, China) mixture at incubator (Thermo Fisher Scientific, USA) with 37 ℃ and 5% CO2.

FVB-MMTV-PyMT mice (Gempharmatech Co., Ltd, China) and FVB mice (Beijing Vital River Laboratory Animal Technology Co., Ltd, China) were fed in SPF laboratory animal rooms which the temperature was 23 ± 3℃, the day and night cycle was alternated for 12 hours. This animal research was reviewed and approved by the Ethics Committee of Ningxia Medical University (license number: SYXK (Ning) 2020-0001).

2.2 Establishment of orthotopic transplantation model of HER2-positive breast cancer in mice

According to Doornebal's research method [21], using FVB-MMTV-PyMT (FVB/N background) mice as donors and FVB/N mice with the same background as recipients, "breast orthotopic tumor transplantation" was performed under Sevoflurane inhalation anesthesia to establish the orthotopic

transplantation model of HER2-positive breast cancer in mice. When the growth of orthotopic breast tumor in recipient mice reached about 2 × 2 mm^3 (defined as "diagnosis time"), the mice were randomly grouped and intervened according to the method of "2.3 Grouping and processing of *in vivo* experiments". When the growth of orthotopic breast tumor in recipient mice reached about 15×15 mm^3 (1687.5 mm^3), the "breast orthotopic transplantation tumor resection" was performed, and the transplanted breast tumor tissues were collected for other experiments (immunohistochemistry, Western blot). Suture the incision, keep warm and supply oxygen during operation. After the operation, the "2.3 Grouping and processing of *in vivo* experiments" method was given to complete postoperative analgesia.

During the post-operation period, disease monitoring was carried out on the recipient mice. When the recipient mice showed painful clinical symptoms caused by metastatic diseases (respiratory distress, abdominal distension, ascites, rapid weight gain, severe anemia, obvious metastatic lesions in lymphatic organs, or local in-situ recurrence of tumor, about 15×15 mm^3), the tumors tissues and organs were collected.

2.3 Experimental grouping and processing *in vivo* and *in vitro*

Cells were randomly divided into control group (C group, RPMI 1640 complete medium only), parecoxib sodium (Pfizer Inc, USA) group (P group, 300 mmol/L), sufentanil (Yichang Humanwell Pharmaceutical Co., Ltd, China) group (SF group, 1 nmol/L [22,23]) and sufentanil + parecoxib sodium combination group (SF+P group, 1 nmol/L + 300 mmol/L). The processing time was 24h.

When the orthotopic breast tumor growth of FVB/N mice reached about 2 × 2 mm^3, the mice were randomly divided into control group (C group, normal saline), parecoxib sodium group (P group, 5 [24]mg/kg), sufentanil group (SF group, 1 μg/kg [25]) and sufentanil + parecoxib sodium combination group (SF+P group, 1 μg/kg +5 mg/kg). The processing was administered by intraperitoneal injection every 12h for 3 consecutive days.

2.4 Substrate adhesion assay

Matrigel matrix gel (Becton, Dickinson and Company, USA) was diluted to 0.04 mg/mL with serum-free RPMI 1640 medium, and 50 mL was added to each well of a 96-well plate, and hydrated in PBS for 60-90 min the next day. BT474 breast cancer cells at logarithmic growth stage were treated according to "2.3 Grouping and processing of *in vitro* experiments". The cells were collected and adjusted to density of $5×10^4$ /well, with 5 replicate wells in each group, and incubated in the incubator for 2 h. The cells were washed with PBS, incubated with 20 mL/well of MTT for 4 h, and then incubated with DMSO 150 mL/well, shaken for 10 min, and the OD value was measured on an enzyme marker at 570 nm. The cell adhesion rate was calculated after 24 h of drug treatment. Cell adhesion rate (%) = (OD experimental group/OD control group) × 100%.

2.5 Wound healing assay

BT474 breast cancer cells in logarithmic growth phase were digested by trypsin (Gibco, 12563011, USA), centrifuged, blown and mixed to make a single cell suspension, inoculated with 2×10^5 cells/well in a 6-well plate. When the cell growth density reached about 70%, intervention was performed according to "2.3 Grouping and processing of *in vitro* experiments". After treatment, the cells in each well were scratched with a 200 mL pipette tip, and the cells were gently washed with PBS solution 3 times after scratching. The marked photographic sites were observed and photographed at 0h and 24h and the wound healing rate was calculated. Wound healing rate (100%) = (0 h area - 24 h area)/0 h area × 100%. The results were analyzed and processed using ImageJ (version 1.52) image software.

2.6 Transwell invasion assay

Matrigel matrix gel was diluted with serum-free RPMI 1640 medium in the ratio of 1:8, and 80 mL was added to each well and incubated at 37 °C for 2 h to solidify into a gel. Mix and suspend BT474 breast cancer cells at logarithmic growth stage with RPMI 1640 medium containing 0.1% FBS, adjust the cell inoculation density to 5×10^5 /well, add 150 mL of cell suspension in the upper chamber of each well and 600 mL of RPMI 1640 complete medium in the lower chamber of each well. The interventions were performed according to "2.3 Grouping and processing of *in vitro* experiments". After treatment, the chambers were fixed with 4% paraformaldehyde for 30 min, washed 3 times with PBS, air-dried upside down, stained with 0.1% crystal violet for 5 min, washed 3 times with PBS, gently wiped off the Matrigel matrix gel and cells on the gel with cotton swabs, dried and observed under an inverted microscope, and the number of membranes piercing cells was counted in 3 randomly selected fields. The results were analyzed and processed by ImageJ (version 1.52) image software.

2.7 Western blot

The total protein was extracted from BT474 breast cancer cells and mice breast cancer tissues, and the concentration of total protein was detected by BCA method (KeyGen Biotech, KGP2100, China). The proteins were separated by SDS-PAGE with a loading volume of 30 μg/well, and the separated proteins on the gel were transferred to PVDF membrane at 270 mA for 2 hours and closed for 2 hours. Wash 3 times with TBST. Add primary antibody Cyclin D1 (1:1000, CST, 55506t, USA), MMP-9 (1:500, Abcam, ab58803, USA), COX-2 (1:3000, Abcam, ab179800, USA), VEGFA (1:200, Abcam, ab1316, USA), E-cadherin (1:1000, Abcam, ab231303, USA), N-cadherin (1:1000, Abcam, ab98952, USA), Vimentin (1:3000, Abcam, ab92547, USA), Snail (1:1000, Abcam, ab180714, USA), and β-actin (1:1000, Proteintech, 20536-1-AP, USA), incubated overnight at 4°C in a shaker. The next day, TBST was washed 3 times and the secondary antibodies of the corresponding species were added and incubated under the chamber for 2 h. After washing 3 times with TBST, the images were developed in a dark room environment using ECL chromogenic solution exposed on a gel imaging system. The results were analyzed and processed using Image Lab (version 6.0.1) image software.

2.8 Growth of mice

FVB/N recipient mice were observed daily from the day of "breast orthotopic tumor transplantation", and the growth of transplanted tumors, diet and feces of the mice were observed. The body weight of the mice was recorded every 3 days, and the longest diameter (A) and the shortest diameter (B) of the transplanted tumor were measured with vernier calipers, and the volume was calculated as $V=1/2 \times A \times B^2$. The survival time of recipient mice was recorded and the survival curve was plotted.

2.9 HE staining

The lung tissues of the mice were fixed with 4% paraformaldehyde, dehydrated by ethanol and embedded in paraffin, then the slices with a thickness of 5 μm were prepared conventionally, dewaxed in xylene and for about 10 ~ 15 min, hydrated by absolute ethanol, 95% ethanol and 80% ethanol in turn for 2 min, dyed with tap water. Hematoxylin nuclear staining for about 5 min, tap water washing, hydrochloric acid ethanol differentiation for 10 s and tap water washing for 30 min. Re-dyeing with 0.5% Eosin for about 2 min, washing with tap water, soaking with 95% ethanol and for 90 s, soaking with absolute ethanol and for 90 s, making xylene and transparent for 10 min, and sealing with neutral gum to dry. Motic digital section scanning and application system (VM1000, China) was used to analyze the images.

2.10 Immunohistochemistry

Paraffin sections of breast cancer tissues were dewaxed and hydrated, and antigen repair was performed with sodium citrate antigen repair solution, goat serum was added and closed at room temperature for 30 min, primary antibody CD31 (1:500, Proteintech, 28083-1-AP, USA), was added and incubated overnight at 4 ℃; the next day, the sections were rewarmed and incubated dropwise with secondary antibody of the corresponding species for 30 min at 37 ℃, washed twice with PBS, DAB staining solution was added dropwise and incubated for 10 min at room temperature, and hematoxylin staining solution was used for restaining. The stains were re-stained with hematoxylin staining solution, dehydrated with ethanol and xylene, sealed with neutral resin, and then photographed under an orthomorphic fluorescence microscope, and the results were analyzed by ImageJ (version 1.52) image software.

2.11 Statistics

Statistical analyses were performed with SPSS 26.0 and GraphPad Prism 9.0 software. The data was expressed in the form of mean ± standard deviation ($\bar{x} \pm s$). Between-group data comparison is conducted by normality test ($P>0.05$) and homogeneity test of variance ($P>0.05$). If the data meet the requirements at the same time, one-way ANOVA is used, and LSD-*t* back testing is used for inter-group comparison. If the data does not meet the normal distribution or variance homogeneity test, the nonparametric rank sum test is selected. The changes of body weight and tumor volume of mice were examined by univariate analysis of variance. Survival analysis was tested by Log-Rank. $P<0.05$, the difference was statistically significant.

3. Results

3.1 Sufentanil combined with parecoxib sodium inhibits the proliferation of BT474 breast cancer cells and induces cell cycle arrest in G1 phase

The proliferation of different groups of cells was detected by CCK8 assay and plate clone formation assay, and the phase distribution of cell cycle was detected by flow cell cycle assay and Western blot. CCK8 assay suggested that parecoxib sodium could inhibit the proliferation of BT474 breast cancer cells, with IC_{50} of 299.5 μmol/L (Fig 1a), and different groups inhibited cell proliferation in a dose-and time-dependent manner, among which the combination group treated for 24h was the most significant (Fig 1b, c). The result of plate formation assay was consistent with CCK8 (fig. 1d). The flow cell cycle assay showed that sufentanil combined with parecoxib sodium increased the G1 phase percentage of BT474 breast cancer cells from 66.83% to 75.01% (Fig 1e), and the expression of G1/S-related protein CyclinD1 was detected by Western blot (Fig 1f, g, h). The results showed that the expression of SF+P decreased. The above experiments suggested that sufentanil combined with parecoxib sodium could inhibit the proliferation of BT474 breast cancer cells and induce cell cycle arrest in G1 phase.

3.2 Sufentanil combined with parecoxib sodium can inhibit the migration and invasion of BT474 breast cancer cells.

The effect of s sufentanil combined with parecoxib sodium on the migration and invasion ability of BT474 breast cancer cells was investigated by scratch assay and transwell invasion assay, and the results of showed that the wound healing rate and invaded numbers of BT474 breast cancer cells in the SF+P group were reduced (Fig 2 a, b). Western blot assay showed that the expression levels of MMP-9, MMP-2 and VEGFA proteins were reduced in the SF+P group (Fig 2c). In addition, the protein related to epithelial-mesenchymal transition (EMT) signaling pathway was detected by Western blot experiment, and it was found that the cell epithelial phenotypic protein E-cadherin was up-regulated and the interstitial phenotypic proteins N-cadherin, Vimentin and Snail were down-regulated in the SF+P group (Figure 2d). It was suggested that sufentanil combined with parecoxib sodium could inhibit the ability to suppress the migration and invasion of BT474 breast cancer cells.

3.3 Sufentanil combined with parecoxib sodium inhibits the growth and metastasis of breast cancer *in vivo*.

The effect of sufentanil combined with parecoxib sodium on the growth and metastasis of breast cancer was further studied by constructing an orthotopic transplantation model of HER2-positive breast cancer in mice (Fig 3), and the intervention was carried out according to the method of "2.3 Grouping and processing of *in vivo* experiments". The results showed that compared with other groups, the weight gain of mice in the SF+P group was less affected (Fig 4a), the tumor-bearing rate of mice increased (Fig 4c) and the survival time was prolonged (Fig 4d). HE staining and immunohistochemical staining showed that the number of lung metastatic nodules (Fig 5a) and the expression of CD31 decreased in breast cancer tissues of mice in the SF+P group (Fig 5b). Western blot assay suggested that sufentanil combined with parecoxib sodium could down-regulate the expression of MMP-9, COX-2 and VEGFA

protein in breast cancer tissues (Fig 5c). At the same time, EMT-related proteins were detected in breast cancer tissues of mice, and it was found that the expression of E-cadherin protein was up-regulated and the expression of N-cadherin, Vimentin and Snail protein were down-regulated to inhibit the occurrence of EMT in breast cancer tissues of mice (Fig. 5d).

4. Discussion

Sufentanil [26,27] combined with parecoxib sodium [28,29] has been reported to be involved in the regulation of biological processes, including tumor cell proliferation, migration and invasion. We performed functional assays to examine the effects of sufentanil combined with parecoxib sodium on HER2-positive breast cancer cells *in vitro* and *in vivo*. BT474 cells are a representative strain of HER2-positive breast cancer cells [30], while MMTV-PyMT spontaneous breast cancer mice (donor) showed HER2-positive phenotypic features by immunophenotyping [21,31]. We found that sufentanil combined with parecoxib sodium induced BT474 breast cancer cells to stagnate in G1 phase and inhibited cell proliferation, migration and invasion. In addition, sufentanil combined with parecoxib sodium inhibited tumor growth and metastasis in HER2-positive breast cancer orthotopic transplantation model mice. The results suggest that sufentanil combined with parecoxib sodium has antitumor effects on HER2-positive breast cancer cells.

Malignant proliferation is not only the basic characteristics of tumor cells but also the focus of tumor prevention and treatment. The concentration of sufentanil (1 nmol/L) used in this study was based on the Bundscherer [22] and Jiang's [23] results, and the concentration and treatment time of this study were initially established based on the effect of CCK-8 assay. The selected drug concentrations and treatment times were further confirmed by combining plate clone formation assay, flow cytometry and Western blot assay. The results showed that sufentanil combined with parecoxib sodium significantly inhibited the proliferation of BT474 breast cancer cells. According to Western Blot results, sufentanil combined with parecoxib sodium inhibited the expression of CyclinD1 protein in cells, promoting G1 phase into S phase. All of these findings support the notion that sufentanil combined with parecoxib sodium inhibits the proliferation of BT474 breast cancer cells.

Invasion and metastasis are the main causes of recurrence and poor prognosis in patients with malignant tumors. Tumor cell invasion and metastasis consist of the following steps: tumor neovascularization [32], extracellular matrix degradation, and tumor cell migration [33,34]. In this study, we found that sufentanil combined with parecoxib sodium caused downregulation of COX-2 and VEGFA protein expression in BT474 breast cancer cells by Western blot assay, suggesting its ability to inhibit tumor blood vessel formation. The effects of sufentanil combined with parecoxib sodium on the chemotaxis and basement membrane penetration of BT474 breast cancer cells were determined by scratch assay and transwell invasion assay, and the results revealed that sufentanil combined with parecoxib sodium had the ability to reduce the migration and invasion of breast cancer cells, suggesting that sufentanil combined with parecoxib sodium has the potential function to inhibit the metastasis of

breast cancer cells. Western blot assay showed that the expression of MMP-9 protein was down-regulated in BT474 breast cancer cells treated with sufentanil with parecoxib sodium, which was consistent with the results of stromal adhesion assay, wound healing assay and transwell assay. EMT is a key step in local tumor infiltration and metastasis to distant organs [35], which affects the malignant biological behavior of tumor cells; therefore, inhibition of EMT occurrence in tumor cells is an important means to reduce tumor recurrence and metastasis. This study detected the expression of EMT-related proteins in treated BT474 breast cancer cells using Western blot, and the results showed that it could inhibit the occurrence of EMT in BT474 breast cancer cells with the ability to enhance intercellular adhesion and reduce cell motility, suggesting that the inhibition of metastasis in BT474 breast cancer cells by sufentanil combined with parecoxib sodium may be related to the inhibition of EMT transformation. The results of this part of the experiment all confirmed that sufentanil combined with parecoxib sodium significantly inhibited the metastatic ability of BT474 breast cancer cells, which may be beneficial for the prevention and treatment of early metastasis of breast cancer.

In vivo, the effects of sufentanil combined with parecoxib sodium on the growth and metastasis of breast cancer were studied. By establishing the orthotopic transplantation model of HER2-positive breast cancer mice and testing the related growth and metastasis functional indexes, it was found that sufentanil combined with parecoxib sodium could not only inhibit the tumor growth, but also reduce the number of lung metastasis nodules and the expression of CD31 in breast cancer tissues. The results were consistent with the Western blot detection of MMP-9, COX-2 and VEGFA, which confirmed that sufentanil combined with parecoxib sodium could inhibit the tumor growth and metastasis of HER2-positive breast cancer mice. In addition, EMT-related proteins were also detected. It was found that sufentanil combined with parecoxib sodium inhibited the EMT transformation, thus inhibiting the invasion and metastasis of breast cancer. This result was consistent with the result of the number of lung metastatic nodules of the recipient mice. The experimental results showed that sufentanil combined with parecoxib sodium can inhibit the growth and metastasis of breast cancer *in vivo*, and further verify the results of *in vitro* experiments. It should be noted that when we performed the comparison of tumor volume changes in recipient mice, we found no statistically significant differences between groups, which we consider to be related to the experimental design of this study, since the monitoring of tumor volume in recipient mice was based on the condition that the tumor volume reached approximately 15 × 15 mm^3 (1687.5 mm^3) consistently as an endpoint in this study. Interestingly, by comparing the experimental results of sufentanil *in vitro* and *in vivo*, it is found that there are differences between the two group. Compared with the control group, *in vitro* results show that sufentanil can inhibit the proliferation and metastasis of BT474 breast cancer cells, while *in vivo* results show that sufentanil can promote the growth and metastasis of breast cancer. For example, *in vivo* experiments showed that sufentanil can increase the growth rate of breast cancer mice's body weight and tumor volume and promote EMT transformation of breast cancer tissues. We considered that these differences may be related to factors such as experimental background, cell type, drug concentration and drug delivery mode of *in vitro* and *in vivo* experiments, which are also consistent with different views on the effect of sufentanil on the prognosis of tumor patients [14-16]. However, *in vitro* and *in vivo* experimental results were consistent that sufentanil

combined with parecoxib sodium can inhibit the proliferation and metastasis of breast cancer cells. At the same time, the analysis of *in vivo* results also suggested that sufentanil combined with parecoxib sodium can effectively reduce the adverse reactions caused by sufentanil, and reduce the possibility of recurrence and metastasis. We considered that this may be related to the use of sufentanil *in vivo* to activate COX-2 and promote the expression of PGE2, which was consistent with the research viewpoint of Dali et al [36]. The combination of sufentanil and parecoxib sodium can counteract this tumor-promoting factor and inhibit the tumor growth and metastasis. This also indicates the potential anti-tumor effect of sufentanil combined with parecoxib sodium, and at the same time, it further illustrates the effectiveness and reliability of the combination of sufentanil and parecoxib sodium for perioperative tumor patients, which provides a new direction for clinical application and research.

In summary, this study demonstrated that sufentanil combined with parecoxib sodium could inhibit the proliferation and metastasis of BT474 breast cancer cells through *in vitro* experiments. On this basis, we further demonstrated that sufentanil combined with parecoxib sodium also inhibited the growth and metastasis of breast cancer *in vivo* by constructing orthotopic transplantation model of HER2-positive breast cancer mice, and found that sufentanil combined with parecoxib sodium inhibited the expression of EMT-related proteins that promote breast cancer metastasis. It is suggested that sufentanil combined with parecoxib sodium may be beneficial to the treatment of perioperative breast cancer patients and improve the long-term prognosis, and also provides a theoretical basis for the selection of more appropriate anesthetic drugs in the perioperative period, but the specific mechanism still needs further study.

Declarations

Acknowledgments This work was supported by the Natural Science Foundation of Ningxia (grant number 2021AAC03399). The funding agency was not involved in the design of the study and collection, analysis, and interpretation of data and in writing the manuscript.

Conflict of interest No potential conflicts of interest were disclosed.

Data availability The datasets generated during and/or analysed during the current study are available from the corresponding author on reasonable request.

References

1. Sung H, Ferlay J, Siegel R L, et al. Global cancer statistics 2020: GLOBOCAN estimates of incidence and mortality worldwide for 36 cancers in 185 countries[J]. CA: a cancer journal for clinicians, 2021, 71(3): 209-249.
2. Martínez-Sáez O, Prat A. Current and future management of HER2-positive metastatic breast cancer[J]. JCO oncology practice, 2021, 17(10): 594-604.

3. Mahvi DA, Liu R, Grinstaff MW, et al. Local Cancer Recurrence: The Realities, Challenges, and Opportunities for New Therapies[J] .CA Cancer J Clin, 2018, 68(6): 488-505.
4. Galon J, Pages F, Marincola F M, et al. Cancer classification using the Immunoscore: a worldwide task force[J]. Journal of translational medicine,2012,10(1):205.
5. Tavare A N, Perry N J S, Benzonana L L, et al. Cancer recurrence after surgery: direct and indirect effects of anesthetic agents[J]. International journal of cancer, 2012, 130(6): 1237-1250.
6. Gottschalk A, Sharma S, Ford J, et al. The role of the perioperative period in recurrence after cancer surgery[J]. Anesthesia & Analgesia, 2010, 110(6): 1636-1643.
7. Bovill J G. Surgery for Cancer: Does Anesthesia Matter? [J]. Anesthesia and analgesia, 2010, 110(6):1524-1526.
8. Zhou D Miao CH. Effect of surgery on cancer recurrence and anaesthetic strategy[J]. International Journal of Anesthesiology and Resuscitation,2013, 34(09):808-811.
9. Horowitz M, Neeman E, Sharon E, et al. Exploiting the critical perioperative period to improve long-term cancer outcomes[J]. Nature reviews Clinical oncology, 2015, 12(4): 213-226.
10. Camara O, Kavallaris A, Nöschel H, et al. Seeding of epithelial cells into circulation during surgery for breast cancer: the fate of malignant and benign mobilized cells[J]. World journal of surgical oncology, 2006, 4(1): 1-7.
11. Saito Y, Shimada M, Utsunomiya T, et al. Regulatory T cells in the blood: a new marker of surgical stress[J]. Surgery Today, 2013, 43(6):608-612.
12. Shi H, Chen X, Liu X, et al. National drug utilization trend of analgesics in China: an analysis of procurement data at 793 public hospitals from 2013 to 2018[J]. Journal of Pharmaceutical Policy and Practice, 2021, 14(1): 1-10.
13. Martinez L, Ekman E, Nakhla N. Perioperative opioid-sparing strategies: utility of conventional NSAIDs in adults[J]. Clinical therapeutics, 2019, 41(12): 2612-2628.
14. Jiang H, Wang H, Zou W, et al. Sufentanil impairs autophagic degradation and inhibits cell migration in NCI-H460 *in vitro*[J]. Oncology letters, 2019, 18(6): 6829-6835.
15. Chipollini J, Alford B, Boulware D C, et al. Epidural anesthesia and cancer outcomes in bladder cancer patients: is it the technique or the medication? A matched-cohort analysis from a tertiary referral center[J]. BMC anesthesiology, 2018, 18(1): 1-9.
16. Forget P, Tombal B, Scholtès J L, et al. Do intraoperative analgesics influence oncological outcomes after radical prostatectomy for prostate cancer? [J]. European Journal of Anaesthesiology (EJA), 2011, 28(12): 830-835.
17. Wang R D, Zhu J Y, Zhu Y, et al. Perioperative analgesia with parecoxib sodium improves postoperative pain and immune function in patients undergoing hepatectomy for hepatocellular carcinoma[J]. Journal of Evaluation in Clinical Practice, 2020, 26(3): 992-1000.
18. Wan Z, Chu C, Zhou R, et al. Effects of oxycodone combined with flurbiprofen axetil on postoperative analgesia and immune function in patients undergoing radical resection of colorectal cancer[J].

Clinical Pharmacology in Drug Development, 2021, 10(3): 251-259.

19. Feng X, Lin S Q, Chen Y, et al. Effect of postoperative analgesia with flurbiprofen axetil and sufentanyl on metabolism of surgical patients with intestinal carcinoma[J]. Nan Fang yi ke da xue xue bao= Journal of Southern Medical University, 2007, 27(10): 1567-1569.
20. Guo J G, Zhao L P, Rao Y F, et al. Novel multimodal analgesia regimen improves post-TACE pain in patients with hepatocellular carcinoma[J]. Hepatobiliary & Pancreatic Diseases International, 2018, 17(6): 510-516.
21. Doornebal C W, Klarenbeek S, Braumuller T M, et al. A preclinical mice model of invasive lobular breast cancer metastasis[J]. Cancer research, 2013, 73(1): 353-363.
22. Bundscherer A Malsy M Gebhardt K et al. Effects of ropivacaine, bupivacaine and sufentanil in colon and pancreatic cancer cells *in vitro*[J]. Pharmacological Research, 2015, 95-96:126-131.
23. Jiang H, Wang H, Zou W, et al. Sufentanil impairs autophagic degradation and inhibits cell migration in NCI-H460 *in vitro*[J]. Oncology letters, 2019, 18(6): 6829-6835.
24. Ferreira T, Campos S, Silva M G, et al. The cyclooxigenase-2 inhibitor parecoxib prevents epidermal dysplasia in HPV16-transgenic mice: efficacy and safety observations[J]. International journal of molecular sciences, 2019, 20(16): 3902.
25. Xiang L, Klemcke H G, Wienandt N A, et al. A novel rat model of extremity trauma for prehospital pain management research[J]. Journal of Trauma and Acute Care Surgery, 2018, 85(1S): S49-S56.
26. Tang H, Li C, Wang Y, et al. Sufentanil Inhibits the Proliferation and Metastasis of Esophageal Cancer by Inhibiting the NF-κB and Snail Signaling Pathways[J]. Journal of Oncology, 2021, 2021: 7586100.
27. Peng Y, Yang J, Guo D, et al. Sufentanil postoperative analgesia reduce the increase of T helper 17 (Th17) cells and FoxP3+ regulatory T (Treg) cells in rat hepatocellular carcinoma surgical model: a randomised animal study[J]. BMC anesthesiology, 2020, 20(1): 1-9.
28. Li L Y, Xiao J, Liu Q, et al. Parecoxib inhibits glioblastoma cell proliferation, migration and invasion by upregulating miRNA-29c[J]. Biology Open, 2017, 6(3): 311-316.
29. Wang R D, Zhu J Y, Zhu Y, et al. Perioperative analgesia with parecoxib sodium improves postoperative pain and immune function in patients undergoing hepatectomy for hepatocellular carcinoma[J]. Journal of Evaluation in Clinical Practice, 2020, 26(3): 992-1000.
30. Mondaca J M, Guijarro A C C, Flamini M I, et al. Heregulin-induced cell migration is prevented by trastuzumab and trastuzumab-emtansine in HER2+ breast cancer[J]. Breast Cancer Research and Treatment, 2021, 186(2): 363-377.
31. Duivenvoorden H M, Spurling A, O'Toole S A, et al. Discriminating the earliest stages of mammary carcinoma using myoepithelial and proliferative markers[J]. PLoS One, 2018, 13(7): e0201370.
32. Du Y, Zhang J, Gong L, et al. Hypoxia-induced ebv-circLMP2A promotes angiogenesis in EBV-associated gastric carcinoma through the KHSRP/VHL/HIF1α/VEGFA pathway[J]. Cancer letters, 2022, 526: 259-272.

33. Makrilia N, Kollias A, Manolopoulos L, et al. Cell adhesion molecules: role and clinical significance in cancer[J]. Cancer investigation, 2009, 27(10): 1023-1037.
34. Condeelis J, Pollard J W. Macrophages: obligate partners for tumor cell migration, invasion, and metastasis[J]. Cell, 2006, 124(2): 263-266.
35. Pastushenko I, Blanpain C. EMT transition states during tumor progression and metastasis[J]. Trends in cell biology, 2019, 29(3): 212-226.
36. Tong D, Liu Q, Wang L, et al. The roles of the COX2/PGE2/EP axis in therapeutic resistance[J]. Cancer and Metastasis Reviews, 2018, 37(2): 355-368.

Figures

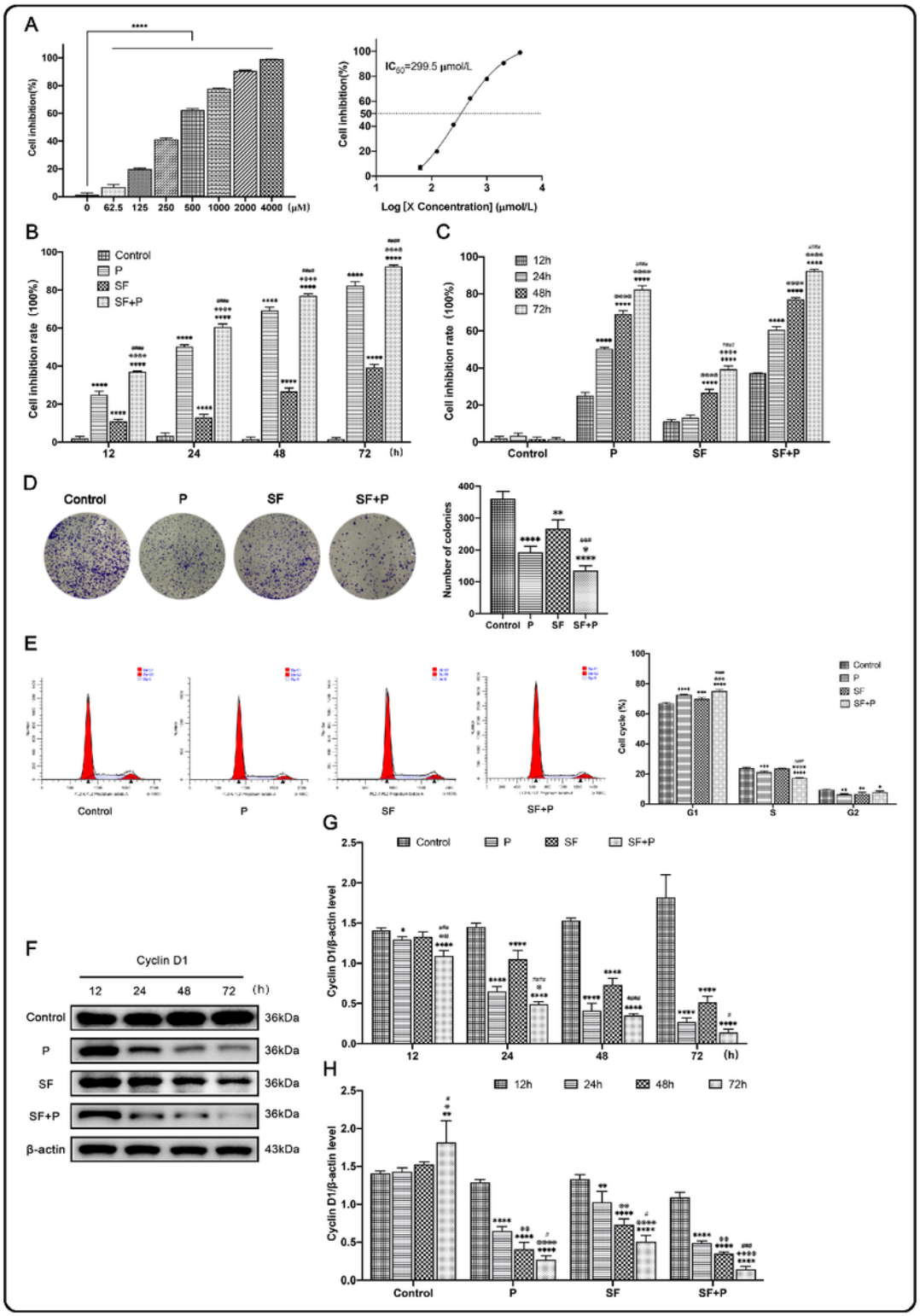

Figure 1

Sufentanil combined with parecoxib sodium inhibits the proliferation of BT474 breast cancer cells and induces cell cycle arrest in G1 phase. **a** Cell proliferation inhibition rate and IC_{50} value of different concentrations of parecoxib sodium after 24h treatment of BT474 breast cancer cells. **b** The inhibition rate of cell proliferation among experimental groups in different time periods. **c** Cell proliferation inhibition rate in each experimental group in different time periods. **d** The results of plate clone forming

ability of each experimental group. **e** results of phase distribution of flow cell cycle in each experimental group. **f** The expression difference of CyclinD1 protein in each experimental group was detected by Western blot (**g** The expression difference of CyclinD1 protein in each experimental group in different time periods. **h** the expression difference of CyclinD1 protein in different experimental groups in different time periods). The data is the average standard deviation of the three independent experiments. (*$^{*}P$*<0.05, *$^{**}P$*<0.01, *$^{***}P$*<0.001, *$^{****}P$*<0.0001 vs Control, $^{※}P$<0.05, $^{※※}P$<0.01, $^{※※※}P$<0.001, $^{※※※※}P$<0.0001 vs P, $^{\#}$P<0.05, $^{\#\#\#}P$<0.001, $^{\#\#\#\#}P$<0.0001 vs SF).

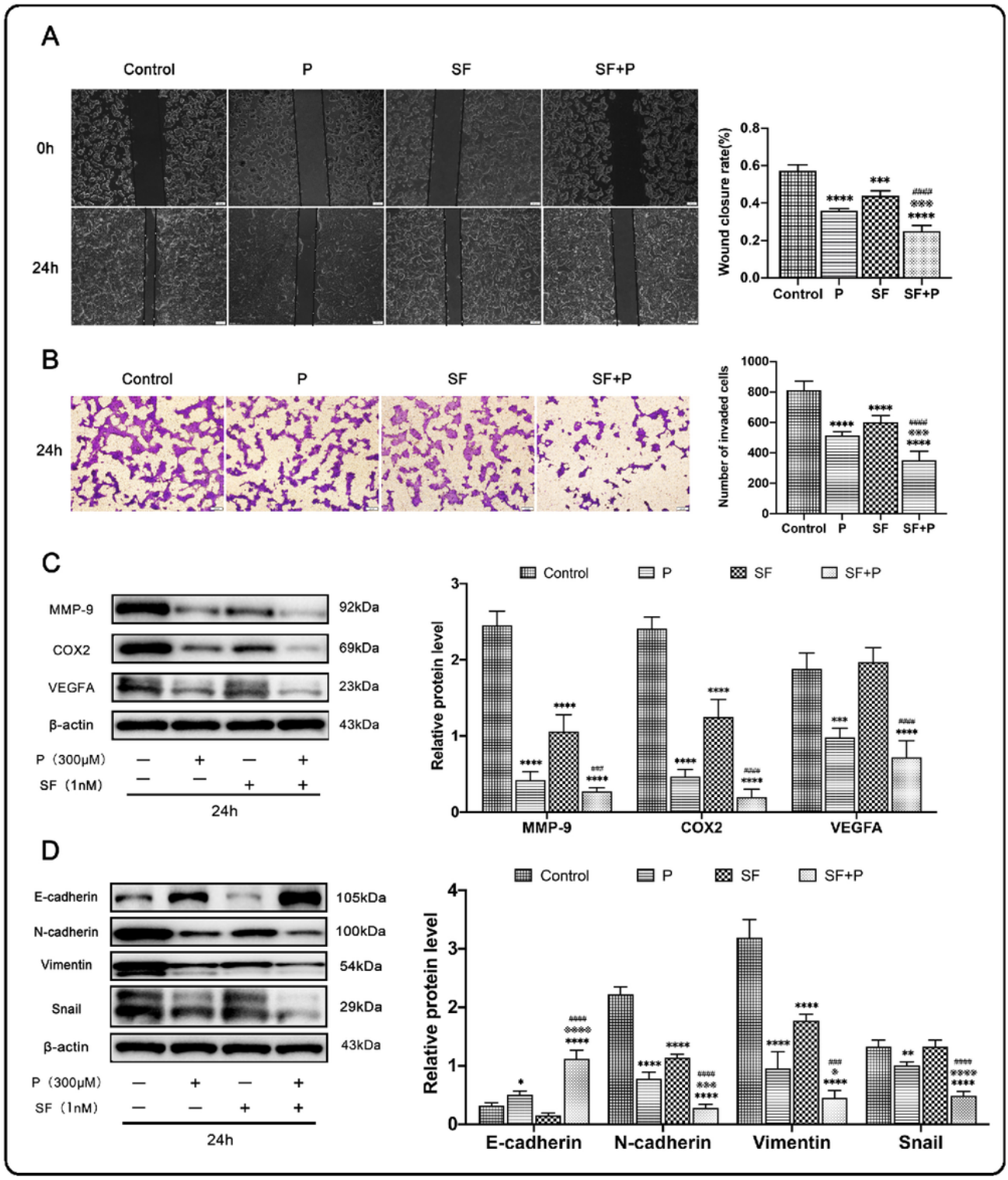

Figure 2

Sufentanil combined with parecoxib sodium inhibits the migration and invasion of BT474 breast cancer cells. **a** Difference of wound healing rate each experimental group, scale =100mm. **b** Difference of invasive cell number in transwell invasion experiment among experimental groups, scale =100mm. **c** The expression of MMP-9, COX-2 and VEGFA in each experimental group was detected by Western blot. **d** The expression difference of EMT-related proteins in each experimental group was detected by Western blot.

The image represents three independent experiments, and the data is the average standard deviation of the three independent experiments. (*P<0.05, **P<0.01, ***P<0.001, ****P<0.0001 vs Control, ※P<0.05, ※※※P<0.001, ※※※※P<0.0001 vs P, ###P<0.001, ####P<0.0001 vs SF).

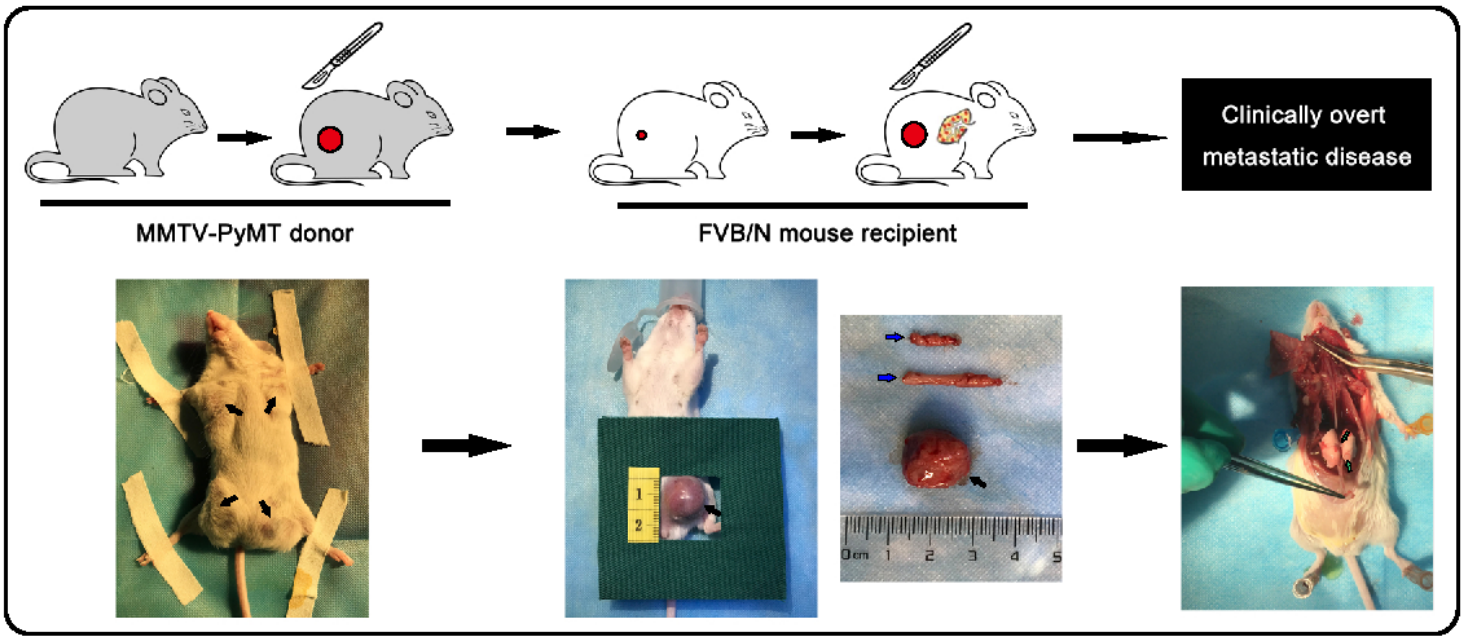

Figure 3

Operation flow chart and schematic diagram of tumor formation and sampling of HER2-positive breast cancer mice orthotopic transplantation model. Black arrow refers to breast orthotopic tumor, blue arrow refers to fourth and fifth breast glands, and green arrow refers to lung metastatic cancer.

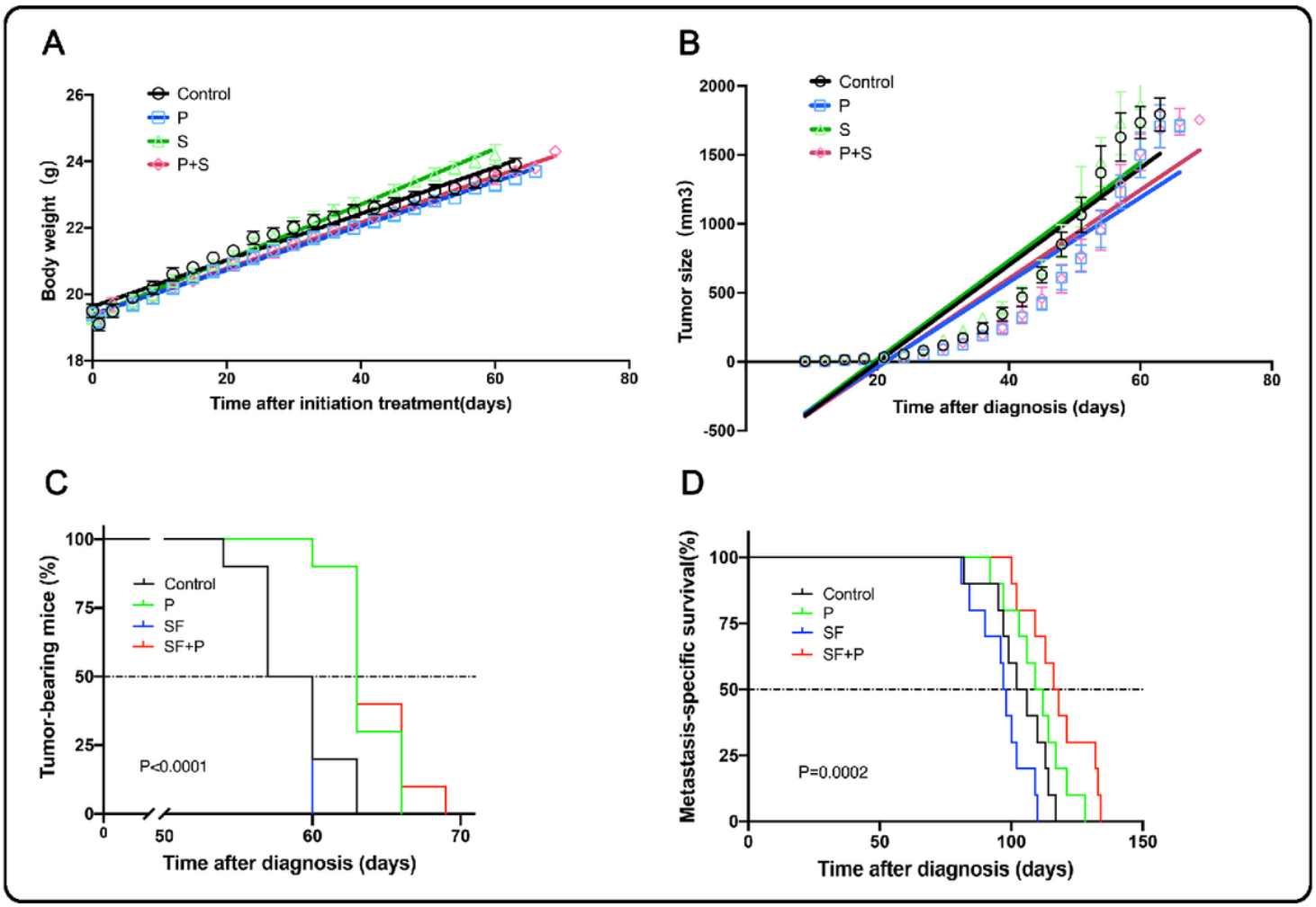

Figure 4

Sufentanil combined with parecoxib sodium inhibits the growth of breast cancer *in vivo*. **a** Curve of weight change of transplanted mice, the weight value of transplanted mice were recorded once every 3 days from the date of " breast orthotopic tumor transplantation", and the time interval ending with " breast orthotopic transplantation tumor resection " $\bar{x}\pm s$ n=10 . **b** The curve of tumor volume of the transplanted mice, the time interval $\bar{x}\pm s$ n=10 from the "diagnosis day" to the end of "breast orthotopic transplantation tumor resection" when the tumor volume of each group reaches about 15×15 mm^3. **c** Kaplan-Meier tumor-related survival curve of the recipient mice, the time interval from the "diagnosis day" to the end of "breast orthotopic transplantation tumor resection" with the tumor volume of each group reaching about 15×15 mm^3, M 95%CI n=10 . **d** Kaplan-Meier survival curve of the recipient mice, the time interval from the date of diagnosis to the time of monitoring the symptoms and signs of metastatic diseases in the recipient mice after the operation of orthotopic breast tumor resection (M(95%CI)), n=10).

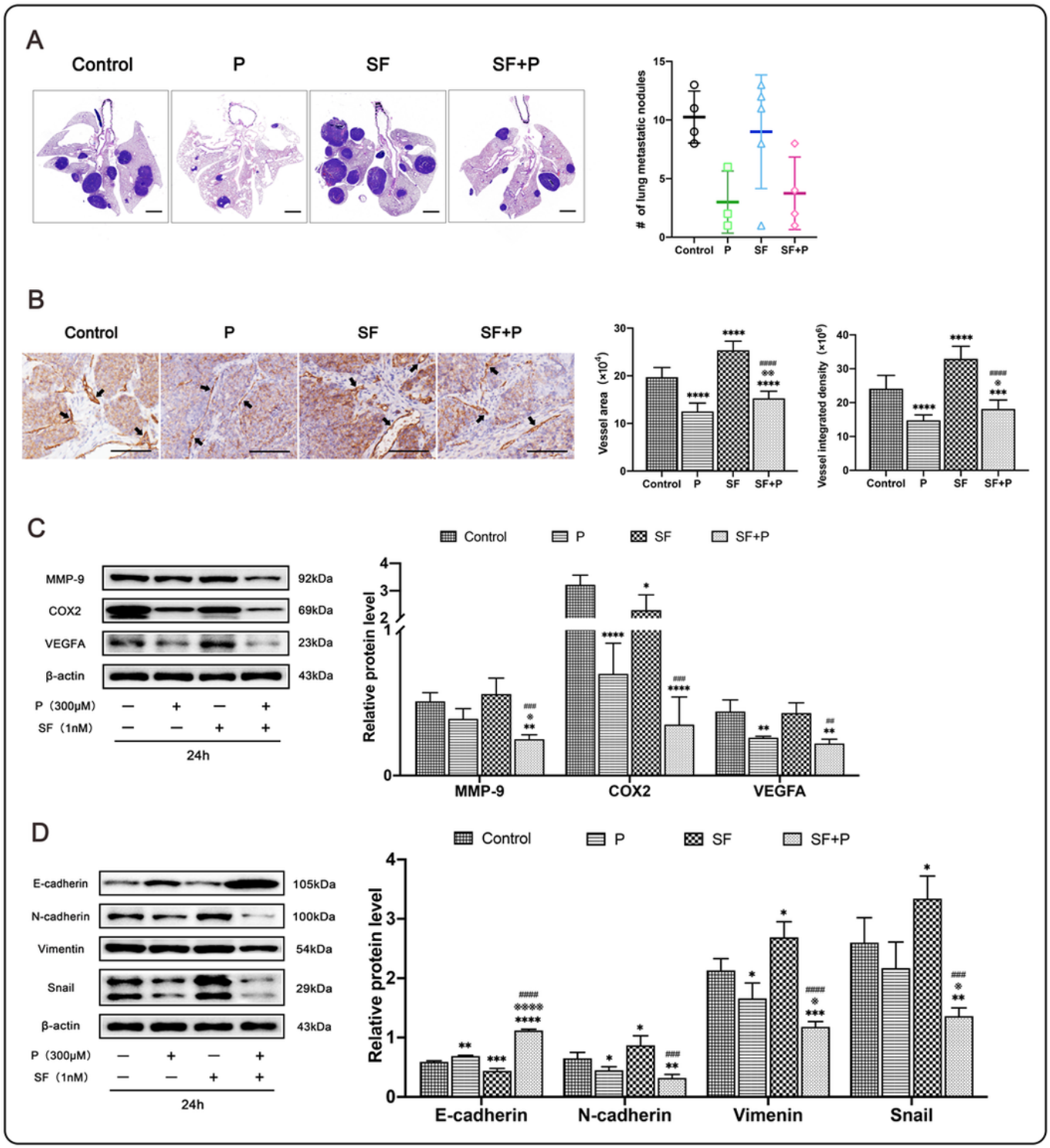

Figure 5

Sufentanil combined with parecoxib sodium inhibits breast cancer metastasis *in vivo*. **a** The representative pictures of HE staining diagram of lung tissue of mice and dot diagram of lung metastasis nodules, scale =500 mm. Control group (n=4), P group (n=3), SF group (n=5), SF+P group (n = 4). **b** Immunohistochemical diagram of CD31 and histogram of blood vessel area and density of blood vessel integration in breast cancer tissues of the transplanted mice. The representative pictures were shown in

the diagram, and the black arrows refer to CD31 positive expression blood vessels, scale =100mm, n=10. **c** The expression of MMP-9, COX-2 and VEGFA in breast cancer tissues of mice in each experimental group, n = 3. **d** The expression difference of EMT-related proteins in breast cancer tissues of mice in each experimental group, n=3. The data is expressed in the form of mean standard deviation. (*P<0.05, **P<0.01, ***P<0.001, ****P<0.0001 vs Control, $^{※}P$<0.05, $^{※※}P$<0.01vs P, $^{※※※※}P$<0.0001 vs P, $^{\#\#}P$<0.01, $^{\#\#\#}P$<0.001, $^{\#\#\#\#}P$<0.0001 vs SF).